

A Nearly Zero-Cost Lot-by-Lot Inspection of Recycled Plastics: Prediction of Mechanical Properties from Viscosity Evolution during Melt Kneading

Yusuke Hibi,* Shiho Uesaka, Kiyotaka Hitomi, Ken-ichi Niihara, Asami Imai, Sadaki Samitsu, and Masanobu Naito*

Cite This: *ACS Sustainable Resour. Manage.* 2025, 2, 673–680

Read Online

ACCESS |

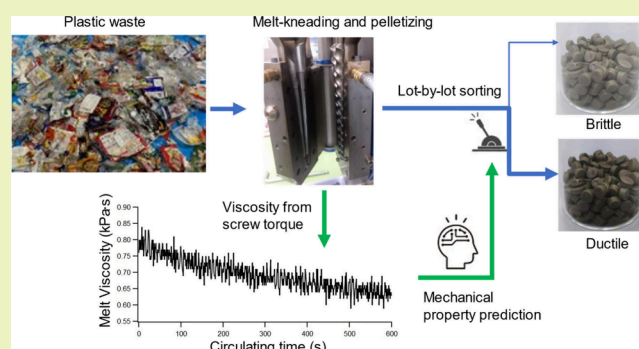
Metrics & More

Article Recommendations

Supporting Information

ABSTRACT: Driving mechanical recycling with minimal energy consumption has become increasingly urgent. However, recycled plastics derived from household plastic waste, which accounts for approximately half of all plastic waste, are contaminated with non-plastic substances and mixed polymers. These contamination levels vary significantly from lot to lot, limiting their use to low-grade applications, where consistent quality is less critical. This study highlights that all recycled plastics undergo melting, kneading, and pelletizing processes. By predicting the mechanical properties of recycled products based on melt viscosity (auxiliary data obtained during kneading without additional costs), we propose a nearly zero-cost, lot-by-lot inspection method. Pre-production prediction of pellet properties during kneading enables the classification and extraction of high-quality, uniform recycled plastics tailored to specific applications. To validate this approach, we predict the tensile properties and Charpy impact energies of 23 lots of household polypropylene (PP) waste. Leveraging a bidirectional recurrent neural network, we developed a system to classify pellets prior to production based on predicted mechanical properties, achieving over 85% accuracy. This innovative analytical method provides a cost-effective solution for upcycling household waste, contributing to sustainability within the circular economy.

KEYWORDS: household plastic waste, mechanical recycling, upcycling, property prediction of recycled materials, melt viscosity, recurrent neural network



INTRODUCTION

Plastic, first commercialized 120 years ago, now contaminates nearly every natural environment. Its environmental impact was already recognized in the 1970s, spurring global efforts to tackle the issue.¹ However, individual ethics and environmental awareness alone are no longer sufficient. Achieving a sustainable society that coexists with plastics requires converting waste into resources. To advance this goal, Plastics Europe has proposed mandating 30% recycled content in plastic packaging by 2030.² Recycled plastics, however, suffer from deteriorated performance due to degradation and contamination. While chemical recycling can restore properties at the molecular level, it is energy-intensive.³ In contrast, mechanical recycling—melting and reusing—offers the lowest global warming impact⁴ and energy-efficient option for plastics with low degradation degree,^{5–7} driving demand for high-quality plastic waste from homogeneous sources like in-factory industrial scrap. Meanwhile, household plastic waste, which is often chemically contaminated,⁸ exhibits significant quality variability depending on the collection time and location. This hinders its use in high-

value applications, leaving household waste as a “lower-grade recycling source”.³

In Japan, household plastic waste accounts for 51% of all plastic waste with only 17% mechanically recycled in 2021.⁹ The 1997 Container and Packaging Recycling Law mandates strict waste separation, allowing Japan to achieve a recycling rate higher than the global average of 9%.¹⁰ However, the quality of recycled materials remains inconsistent,¹¹ driving demand for analytical technologies that can extract high-quality fractions. Property requirements also vary by application such as balancing stiffness and ductility. Lot-by-lot characterization of recycled plastics enables optimal allocation of each lot to suitable applications. However, economic constraints¹² limit such

Received: January 20, 2025

Revised: March 12, 2025

Accepted: March 12, 2025

Published: March 21, 2025



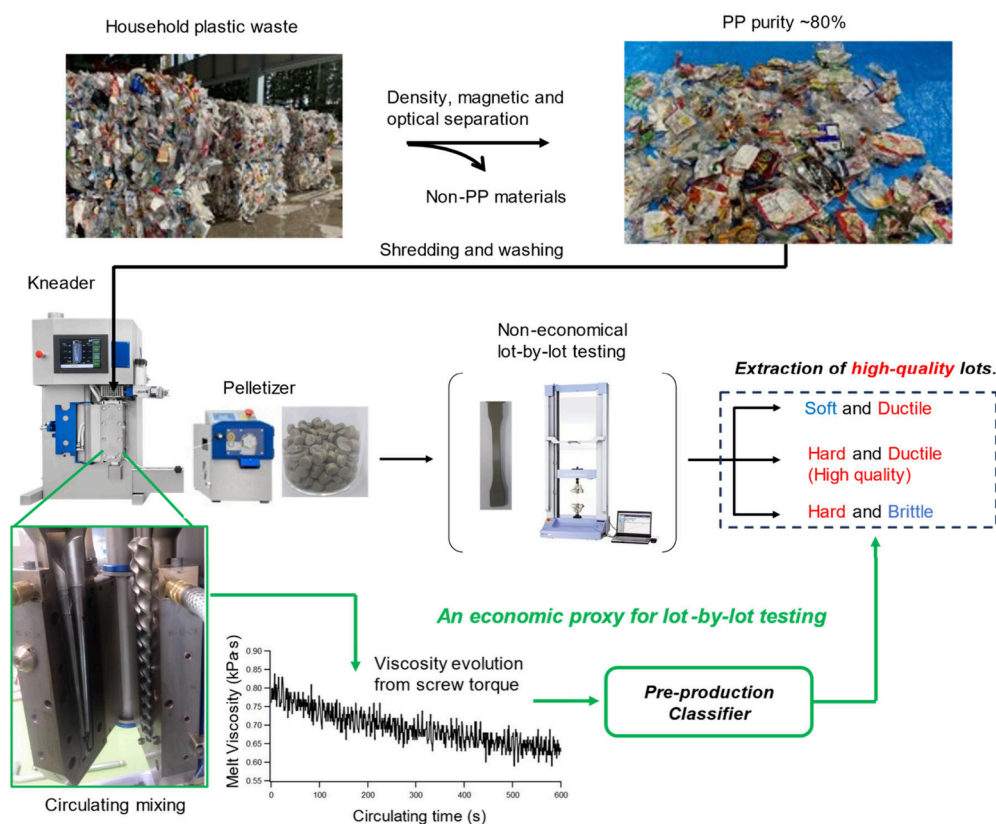


Figure 1. A nearly zero-cost lot-by-lot inspection is achieved by predicting tensile properties based on melt viscosity—auxiliary data obtained without incurring costs—during the pelletizing process of recycled materials.

inspection systems to sorting by color and polymer type using in-line optical separation techniques, such as Raman spectroscopy,¹³ near-infrared spectroscopy (NIR),¹⁴ laser-induced plasma spectroscopy,¹⁵ and hyperspectral imaging.¹⁶

This study highlights that all recycled plastics undergo melting, kneading, and pelletizing processes before entering the recycled materials market. During kneading, the torque required to maintain screw rotation reflects polymer viscosity, enabling cost-free derivation of apparent melt viscosity.¹⁷ Continuous monitoring of viscosity changes reveals the plastic's fluidity response to heat and stress, which typically decreases due to thermal plasticization and degradation.¹⁸ This viscosity evolution could embed lot-specific information, such as molecular weight distribution, chemical degradation, and contamination levels, serving as a cost-free descriptor for predicting mechanical properties of products. By leveraging deep learning techniques,¹⁹ such as bidirectional recurrent neural networks (RNNs),²⁰ the mechanical properties of recycled pellets can be predicted prior to production, enabling the extraction of uniform, high-quality lots (Figure 1). This study further demonstrates that viscosity data collected under one set of thermal conditions can predict the properties of specimens processed under different conditions. This finding has significant practical implications, as viscosity data from pelletization can predict the properties of products manufactured by reprocessing the pellets under different conditions. This enables the extraction of optimal lots tailored to customer-specific applications, promoting upcycling.

EXPERIMENTAL SECTION

Melt Kneading for Viscosity Data Acquisition and Tensile Test Specimen Preparation. The dataset used in this study

comprises 23 samples of polypropylene (PP) derived from household waste, collected on different days between April and June 2023 from various local governments in Japan. The samples were presorted by density, magnetic, and optical separations and subsequently compacted into pellets, following the industrial recycling process of Toyama Kankyo Seibi Co., Ltd. The resulting recycled plastics of roughly 11.5 g were then loaded into a small twin-screw extruder with a circulating path (Xplore MC 15HT; Xplore Instruments) at 220 °C for 600 seconds. The melting point of PP is typically around 160 °C, and 220 °C may seem relatively high. However, there are two key reasons for using a high temperature. First, the high-throughput processing of large volumes of recycled plastic requires higher temperatures to reduce viscosity and ensure efficient mixing. Second, high-temperature kneading helps reset the polymer chain conformation, which is believed to improve mechanical properties.²¹ The screw speed was fixed at 100 rounds per minute, and from the necessitated torque current, the melt viscosity was calculated by default software equipped in Xplore MC 15HT. After the mixing, the melt plastics were injected into a dog-bone mold by air pressure of 6 bar at 45 °C, yielding two dog-bone-shaped specimens. The resulting specimens were then subjected to a tensile test.

Tensile Testing. Tensile testing was conducted by using AG-10KNX (Shimadzu). The tensile speed was fixed at 30 mm/min. Since melt-kneading mentioned above could afford only three specimens, one of them is contaminated with the previous melt-kneading sample, and only two trials per one recycled PP could be conducted. However, as shown in Figure 2, the two stress–strain curves for identical samples were well consistent including breaking stress. From each curve, elastic modulus, yield strength, and breaking stress were calculated using the equipped software and averaged over two trials for a single sample, as summarized in Table S1.

Charpy Impact Testing. The Charpy impact test specimens were prepared using a single-screw extruder with a linear pathway at 250 °C. The kneading time is constant, as it corresponds to the time required for the molten plastic to pass through the linear pathway, but it remains

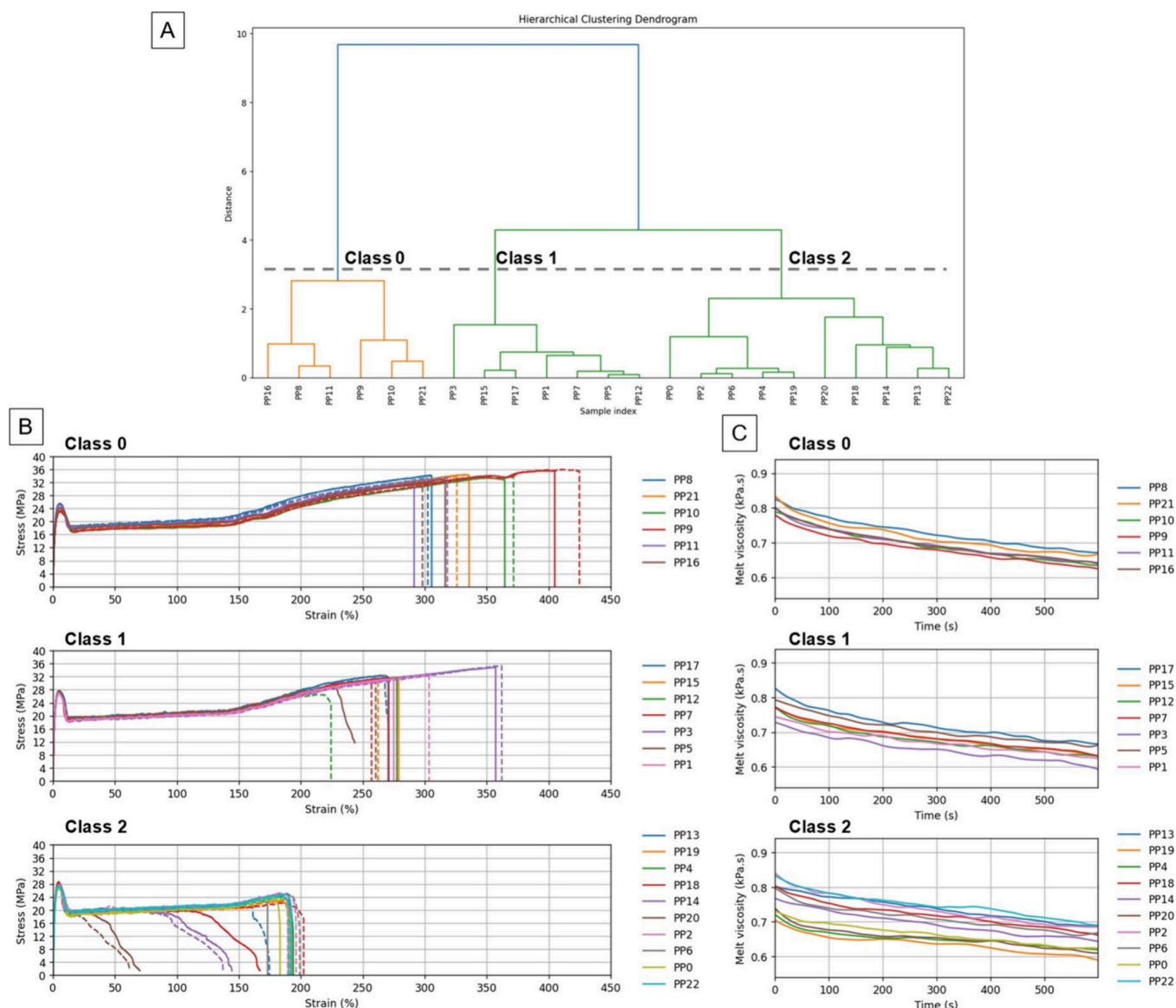


Figure 2. (A) Class labeling based on hierarchical clustering of the tensile properties of the 23 types of recycled materials. (B) Tensile tests were performed for each class. Two tensile tests were conducted for each recycled material, with the first test shown by a solid line and the second by a dashed line in the same color. The repeated curves were consistent, including breaking stress. (C) Smoothed melt viscosity data were obtained for each class.

unknown. The test specimens were molded into rectangular bars ($80 \times 10 \times 4$ mm) using an EC30SXII-1A injection molding machine (Shibaura Machine Co., Ltd.) at a molding temperature of 230 °C. Notches were introduced using a notching tool (model A-4E; Toyo Seiki Seisakusho, Ltd.). The impact tests were conducted using a 2 J hammer at 23 °C, with each test repeated five times, and the average impact energies were recorded and summarized in Table S1.

RESULTS AND DISCUSSION

In practical pelletizing, product pellets should be classified based on pre-production property predictions. Accordingly, 23 recycled materials were grouped into three classes via hierarchical clustering based on tensile properties, and class labels were assigned to the corresponding melt viscosity curves (Figure 2A and Table S1). Class 0 had a low elastic modulus (830 ± 39 MPa) and yield stress (24.0 ± 1.08 MPa), but a high breaking strain ($338 \pm 45\%$). Class 2 had a high elastic modulus (987 ± 39 MPa) and yield stress (27.6 ± 0.49 MPa), but a low

breaking strain ($171 \pm 41\%$), indicating hardness but brittleness. Class 1, representing “high-quality” PP, showed a balanced profile with a high elastic modulus (943 ± 13 MPa) and yield stress (27.2 ± 0.27 MPa) and moderate breaking strain ($279 \pm 37\%$).

The melt viscosity curves in Figure 2C lack distinct class-specific features. To enhance them, we applied mathematical preprocessing (Figure 3). Given the small dataset and the need to simplify the model, the data were averaged every 20 s, reducing 600 time points to 30 . The dataset was then standardized to a mean of zero and a variance of one, preserving the relative magnitudes of melt viscosities across samples—an essential characteristic of the “raw data” (Figure 3A). Overlaying the curves with class-specific colors revealed trends in viscosity magnitudes: Class 0 > Class 1 > Class 2. However, substantial intra-class variability and overlap among classes made discrimination challenging. Moreover, melt viscosity derived from the torque is affected not only by the plastic’s intrinsic

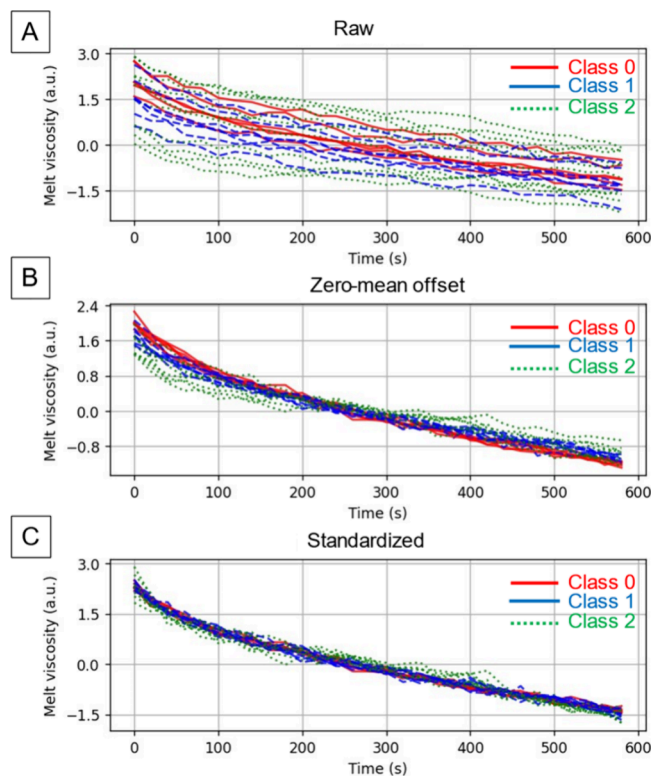


Figure 3. Time evolution curves of melt viscosity during the circulating kneading process. (A) Raw data, (B) zero-mean offset, and (C) standardized data. The colors red, blue, and green represent tensile classes 0, 1, and 2, respectively.

properties but also by external factors such as feed quantity and residuals from previous lots. Therefore, predictive models should account for such uncertainties in viscosity measurements.

To address this, we applied a mean-zero offset adjustment to each sample, aligning the time-series average to zero (Figure 3B). This eliminated relative magnitude differences among samples but enhanced class-specific trends in viscosity changes, particularly in the gap between initial and final viscosities: Class 0 > Class 1 > Class 2. Further standardization of the mean-zero offset data to a variance of one (Figure 3C) emphasized curve

shape, compensating for the lost information on the gap magnitudes. Since each of the three data types—raw, mean-zero offset, and standardized—highlighted distinct features, combining all three as inputs to machine learning models would facilitate mechanical property prediction compared to using raw data alone. Note that the reduction in viscosity over time is generally attributed to a decrease in molecular weight due to thermal degradation.²² However, a recent study indicates that recycled PP does not undergo severe chemical degradation under 210–250 °C for about 10 min.²¹ Instead, because recycled PP generally contains around 20% of other polymers such as polyethylene or polystyrene, both of which are immiscible with PP, morphological changes in these domains can also explain viscosity reduction.²³ Regardless of the mechanism, the initial molecular weight distribution and polymer composition strongly influence how the viscosity evolves. Therefore, using an RNN to analyze viscosity evolution profiles may predict the mechanical properties for each lot.

Figure 4 illustrates the architecture of the predictive model, which outputs logits for the three tensile classes. The class with the highest logit is selected as the predicted class for the corresponding input viscosity data with a dimension of (3, 30), corresponding to three channels of raw, mean-zero offset, and standardized data with 30 timepoints. The last point, reflecting the plastic's condition just before molding, would be critical for property predictions. However, as mentioned above, the temporal evolution of melt viscosity also exhibits distinct class-specific features. Additionally, the rapid response to heat and stress likely reflects the polymer's microenvironment through its thermal stability.²⁴ Therefore, a bidirectional RNN architecture effective for capturing the “context” specifically at the first and last was adopted.²⁰ The extracted “context” of the viscosity evolution is then passed through two fully connected layers, which compute the logits for the three tensile classes. This simple model architecture was specifically designed to accommodate the extremely small dataset. To further address the dataset limitations, we augmented the viscosity curves by randomly adding Gaussian noise, increasing the dataset size tenfold (see Figure S1 for example of augmented viscosity curves).²⁵ The model was optimized by minimizing cross-entropy loss using a learning rate of 0.01 and mini-batch training with 50 batches over 300 epochs.

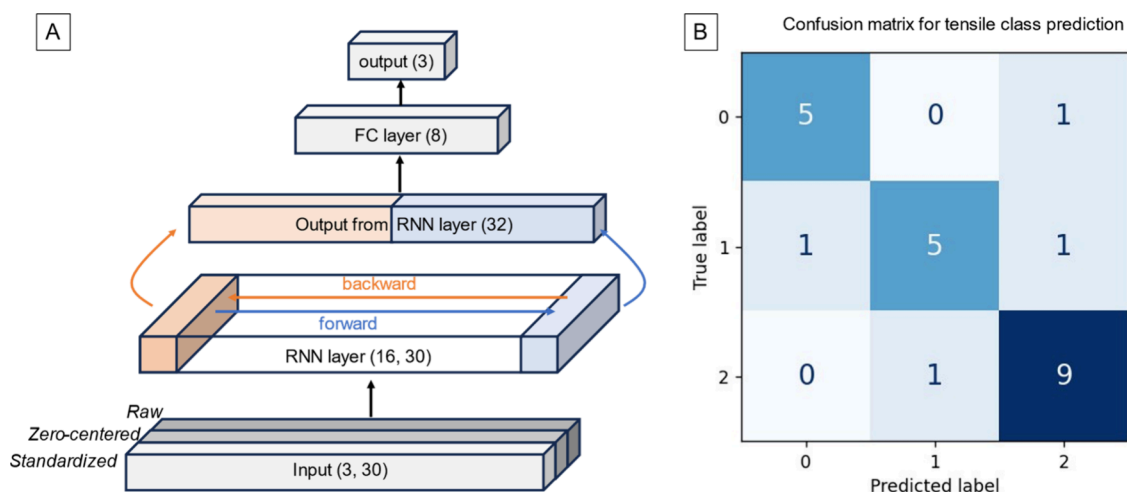


Figure 4. (A) Structure of the RNN class classifier. The numbers represent the dimensions of the network. (B) Confusion matrix showing the results of LOOCV.

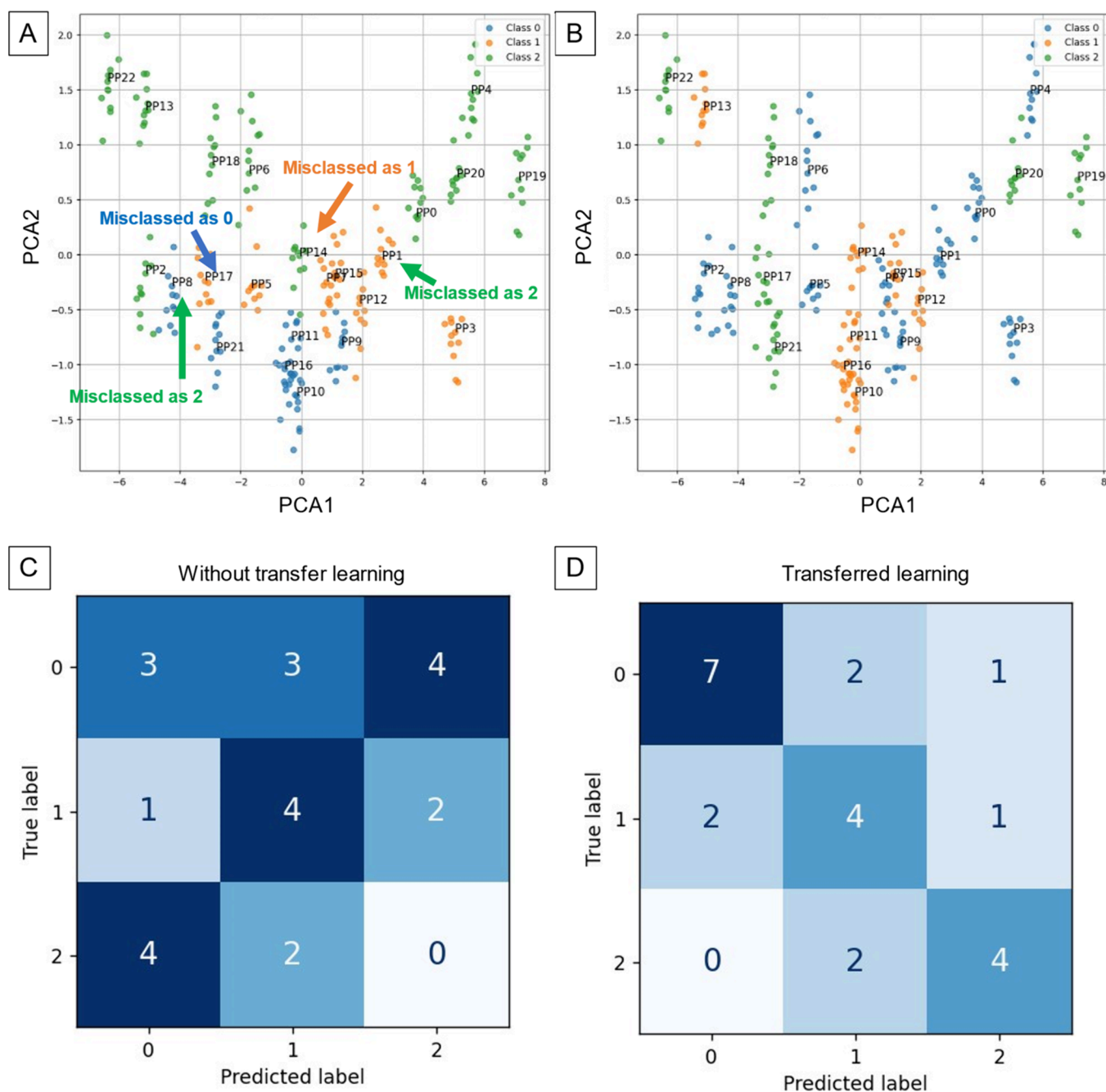


Figure 5. Transfer learning from the tensile prediction model to predict Charpy impact energy. (A and B) Lower-dimensional representations of original and augmented melt viscosity curves obtained using principal component analysis (PCA), colored by tensile classes (A) and impact classes (B). (C and D) Confusion matrices for Charpy impact energy prediction without transfer learning (C) and with transfer learning from the tensile prediction model (D).

The model was implemented using Pytorch (see [Data S2](#) for the source code). Due to the small dataset, we employed leave-one-out cross-validation (LOOCV) to evaluate model accuracy. For each of the 23 iterations, the model was trained on 22 class-labeled viscosity curves, with the remaining curve used as the test input. This process produced the confusion matrix (Figure 4B), showing the true labels on the vertical axis and the predicted labels on the horizontal axis. Each cell indicates how many samples fall into each true–predicted pair. If most samples lie along the diagonal from top-left to bottom-right, then the prediction model is both accurate and highly sensitive. Notably, during LOOCV, both the original test sample and its 10

augmented duplicates were entirely excluded from the training set.

Despite the small dataset, the model achieved over 85% accuracy using all three input channels. In contrast, predictions based on one or two channels were less reliable (Figure S2), highlighting the effectiveness of three-channel inputs in mitigating uncertainties in viscosity curves. To evaluate whether the prediction accuracy was sufficient for extracting high-quality lots, six lots predicted as Class 1 (Figure 4B, middle column) were mixed in equal proportions, kneaded, and tested for tensile properties. Of these six lots, five were true Class 1, while one was a relatively brittle Class 2. The resulting elastic modulus, yield

stress, and breaking strain were 930 MPa, 26.1 MPa, and 283%, respectively—closely matching the average values of true Class 1 samples. This confirmed that the prediction accuracy was sufficient to enable cost-effective extraction of high-quality lots without full-lot inspection. The four misclassified samples in Figure 4B are marked in the lower-dimensional descriptor space in Figure 5A. Misclassifications were observed near the boundary where the three classes converge, a common challenge in multi-class classification. This issue can be mitigated by increasing the density of samples near the boundary.

We extended the melt viscosity-based prediction model to include the Charpy impact energy. Unlike tensile test specimens, which were molded immediately after the viscosity data were recorded from the same lot portion, Charpy test specimens were prepared from a separate portion using a single-screw kneader under distinct conditions. This discrepancy introduced complexity as the melt viscosity data did not reflect the thermal history of the Charpy specimens. The increased complexity is evident in the lower-dimensional visualization of the melt viscosity curves (Figures 5A and 5B) generated by principal component analysis (PCA). In this analysis, the original high-dimensional dataset (3×30) was projected onto a two-dimensional space defined by the first two principal components (PCA1 and PCA2). These components capture the greatest variance in the data, providing an optimal lower-dimensional representation, while preserving key structural patterns.

The projected data points are colored by the tensile classes in Figure 5A and by the Charpy impact energy classes in Figure 5B. Notably, the tensile classes formed distinct clusters, whereas the impact energy classes did not. This suggests that when two lots exhibit broadly similar viscosity profiles, they also tend to have similar tensile properties—indicating that tensile classes can be predicted relatively easily. In contrast, the absence of well-defined clustering by Charpy impact classes implies that simply examining broad viscosity patterns may be insufficient for predicting impact energy classes. Instead, subtle details of the viscosity profile—or potentially strong nonlinearities between viscosity and Charpy properties—become important, making accurate impact predictions significantly more challenging.

For Charpy impact testing, samples were classified into three classes—Classes 0, 1, and 2—based on impact energy from lowest to highest (see Table S1 for numerical data and Figure S3 for labels). Unlike tensile classification based on three properties, the impact classification is based on scalar values with a clear ordinal relationship. To reflect class distances, we employed label distribution learning²⁶ with soft labels instead of one-hot encoding (e.g., [1, 0, 0] for Class 0). The soft labels were approximately defined based on a Gaussian distribution, assuming a class-to-class distance of 0.7 sigma, as follows: Class 0, [0.75, 0.2, 0.05]; Class 1, [0.2, 0.6, 0.2]; and Class 2, [0.05, 0.2, 0.75]. This approach accounts for both class distances and uncertainty in label assignment, making it particularly effective for datasets like impact energy, where standard deviations are comparable to class thresholds (see Figure S3). The loss function was defined using Kullback–Leibler divergence between predicted probabilities and soft labels. Other than label representation, the model architecture remained identical to that used for tensile property prediction.

Direct prediction of impact classes from viscosity data resulted in unsatisfactory accuracy and sensitivity (Figure 5C). In particular, brittle Class 0 specimens were frequently misclassified as impact-resistant Class 2, failing to exclude defective lots and maintain product quality. To address this, we

employed transfer learning,²⁷ reusing RNN layers pre-trained for tensile prediction and fine-tuning the fully connected layers for impact prediction (Figure 5D; see Figure S4 for the flowchart). This approach improved the sensitivity to 70% for detecting brittle Class 0 (7/10) and achieved 66% accuracy for impact-resistant Class 2 (4/6). Notably, only one defective Class 0 sample was misclassified as Class 2, demonstrating sufficient accuracy to prevent quality and pricing downgrades. Pre-training on tensile classification enabled the RNN to extract lot-specific features from viscosity data, allowing for property prediction despite the weak correlation between viscosity and Charpy class, which arises from the different thermal conditions used during specimen preparation, as mentioned earlier.

CONCLUSION

This study explored a nearly zero-cost lot-by-lot inspection method for recycled PP. Implementing this approach in recycling facilities would readily expand the dataset, enhancing predictive accuracy and enabling the use of advanced models, such as attention-based models,²⁸ to investigate the links between mechanical properties and melt viscosity. Integrating chemical spectrometry techniques, like Raman spectroscopy,¹³ NIR,¹⁴ and pyrolysis mass spectrometry,^{29–32} with mechanical viscosity data would provide deeper insights into multi-component polymer systems and their interactions,³³ enabling predictions of more advanced properties.

While actual recycling facilities typically use linear kneaders instead of circulating ones, time-dependent changes in viscosity can be interpreted as continuous viscosity changes along the kneading path, which can be monitored using embedded soft sensors.³⁴ Such soft sensors offer higher accuracy than torque-derived viscosity, deriving more reliable descriptors. Additionally, the recycled PP used in this study was primarily sourced from food packaging, which generally contains minimal additives or fillers. While some contamination may be present, its level is likely low. Therefore, we cannot directly claim that the proposed model is applicable to PP samples with a high filler or additive content. However, since such additives and fillers significantly influence viscosity evolution, the viscosity profile likely contains implicit information about their presence. This suggests that it may be possible to predict material properties influenced by fillers and additives. Overall, the cost-effective lot-by-lot inspection technique would significantly advance the circular economy.

ASSOCIATED CONTENT

Supporting Information

The Supporting Information is available free of charge at <https://pubs.acs.org/doi/10.1021/acssusresmgt.5c00040>.

Numerical physical properties of the 23 PP lots used in this study and Figures S1–S4 (PDF)

Raw stress–strain curve and viscosity profile data (Data S1) (ZIP)

Source code for model implementation (Data S2) (TXT)

AUTHOR INFORMATION

Corresponding Authors

Yusuke Hibi – Data-Driven Polymer Design Group, Research Center for Macromolecules and Biomaterials, National Institute for Materials Science (NIMS), Tsukuba, Ibaraki 305-0047, Japan; orcid.org/0000-0003-4006-1070; Email: hibi.yusuke@nims.go.jp

Masanobu Naito – Data-Driven Polymer Design Group, Research Center for Macromolecules and Biomaterials, National Institute for Materials Science (NIMS), Tsukuba, Ibaraki 305-0047, Japan; orcid.org/0000-0001-7198-819X; Email: naito.masanobu@nims.go.jp

Authors

Shiho Uesaka – Data-Driven Polymer Design Group, Research Center for Macromolecules and Biomaterials, National Institute for Materials Science (NIMS), Tsukuba, Ibaraki 305-0047, Japan

Kiyotaka Hitomi – Data-Driven Polymer Design Group, Research Center for Macromolecules and Biomaterials, National Institute for Materials Science (NIMS), Tsukuba, Ibaraki 305-0047, Japan

Ken-ichi Niihara – Toyama Kankyo Seibi, Toyama 939-2638, Japan

Asami Imai – Toyama Kankyo Seibi, Toyama 939-2638, Japan

Sadaki Samitsu – Data-Driven Polymer Design Group, Research Center for Macromolecules and Biomaterials, National Institute for Materials Science (NIMS), Tsukuba, Ibaraki 305-0047, Japan; orcid.org/0000-0002-4139-1656

Complete contact information is available at:

<https://pubs.acs.org/10.1021/acssusresmgmt.5c00040>

Author Contributions

Y.H. conceived the research, designed the experiment, developed the software, analyzed the data, wrote the manuscript, and supervised the project. S.U. conducted melt-kneading and tensile testing. K.N. and A.I. prepared recycled PPs and conducted Charpy impact testing. K.H. and M.N. installed and setup the twin-screw extruder. S.S. input his idea into the project.

Funding

This work was supported by JSPS KAKENHI Grant JP24K08520 (to Y.H.) and the Cross-Ministerial Strategic Innovation Promotion Program (SIP) JPJ012290 (to M.N.).

Notes

The authors declare the following competing financial interest(s): The authors are owners of potential patent applications.

REFERENCES

- (1) Sighicelli, M.; Pietrelli, L.; Lecce, F.; Iannilli, V.; Falconieri, M.; Coscia, L.; Di Vito, S.; Nuglio, S.; Zampetti, G. Microplastic Pollution in the Surface Waters of Italian Subalpine Lakes. *Environ. Pollut.* **2018**, *236*, 645–651.
- (2) Lase, I. S.; Tonini, D.; Caro, D.; Albizzati, P. F.; Cristóbal, J.; Roosen, M.; Kusenberg, M.; Ragaert, K.; Van Geem, K. M.; Dewulf, J.; De Meester, S. How Much Can Chemical Recycling Contribute to Plastic Waste Recycling in Europe? An Assessment Using Material Flow Analysis Modeling. *Resour. Conserv. Recycl.* **2023**, *192*, No. 106916.
- (3) Civancik-Uslu, D.; Nhu, T. T.; Van Gorp, B.; Kresovic, U.; Larrain, M.; Billen, P.; Ragaert, K.; De Meester, S.; Dewulf, J.; Huysveld, S. Moving from Linear to Circular Household Plastic Packaging in Belgium: Prospective Life Cycle Assessment of Mechanical and Thermochemical Recycling. *Resour. Conserv. Recycl.* **2021**, *171*, No. 105633.
- (4) Huysveld, S.; Ragaert, K.; Demets, R.; Nhu, T. T.; Civancik-Uslu, D.; Kusenberg, M.; Van Geem, K. M.; De Meester, S.; Dewulf, J. Technical and Market Substitutability of Recycled Materials: Calculating the Environmental Benefits of Mechanical and Chemical

Recycling of Plastic Packaging Waste. *Waste Management* **2022**, *152*, 69–79.

(5) Lange, J. P. Managing Plastic Waste-Sorting, Recycling, Disposal, and Product Redesign. *ACS Sustain. Chem. Eng.* **2021**, *9* (47), 15722–15738.

(6) Hibi, Y.; Matsumoto, T.; Midorikawa, M.; Uesaka, S.; Mizoshiri, M.; Tanimura, T.; Okada, M.; Naito, K.; Naito, M. Defining the Degree of Degradation in Plastics: Quantification of Accumulated Degradation Products and Leached Stabilizers for Predicting End-of-Life. *Polym. Degrad. Stab.* **2025**, *232*, No. 111128.

(7) Tigner, J. M.; Elmer-Dixon, M. M.; Maurer-Jones, M. A. Quantification of Polymer Surface Degradation Using Fluorescence Spectroscopy. *Anal. Chem.* **2023**, *95* (26), 9975–9982.

(8) Su, Q. Z.; Vera, P.; Nerín, C. Combination of Structure Databases, In Silico Fragmentation, and MS/MS Libraries for Untargeted Screening of Non-Volatile Migrants from Recycled High-Density Polyethylene Milk Bottles. *Anal. Chem.* **2023**, *95* (23), 8780–8788.

(9) PWMI Newsletter 1 Plastic Products, Plastic Waste and Resource Recovery, 2021. https://www.pwmi.or.jp/ei/siryoy/ei/ei_pdf/ei52.pdf (accessed 2024-12).

(10) Geyer, R.; Jambeck, J. R.; Law, K. L. Production, Use, and Fate of All Plastics Ever Made. *Sci. Adv.* **2017**, *3* (7), n/a.

(11) Ragaert, K.; Delva, L.; Van Geem, K. Mechanical and Chemical Recycling of Solid Plastic Waste. *Waste Management* **2017**, *69*, 24–58.

(12) Van Camp, N.; Lase, I. S.; De Meester, S.; Hoozée, S.; Ragaert, K. Exposing the Pitfalls of Plastics Mechanical Recycling through Cost Calculation. *Waste Management* **2024**, *189*, 300–313.

(13) Saerens, L.; Vervaeke, C.; Remon, J. P.; De Beer, T. Visualization and Process Understanding of Material Behavior in the Extrusion Barrel during a Hot-Melt Extrusion Process Using Raman Spectroscopy. *Anal. Chem.* **2013**, *85* (11), 5420–5429.

(14) Bashirgonbadi, A.; Saputra Lase, I.; Delva, L.; Van Geem, K. M.; De Meester, S.; Ragaert, K. Quality Evaluation and Economic Assessment of an Improved Mechanical Recycling Process for Post-Consumer Flexible Plastics. *Waste Management* **2022**, *153*, 41–51.

(15) Fink, H.; Panne, U.; Niessner, R. Process Analysis of Recycled Thermoplasts from Consumer Electronics by Laser-Induced Plasma Spectroscopy. *Anal. Chem.* **2002**, *74* (17), 4334–4342.

(16) Henriksen, M. L.; Karlsen, C. B.; Klarskov, P.; Hinge, M. Plastic Classification via In-Line Hyperspectral Camera Analysis and Unsupervised Machine Learning. *Vib. Spectrosc.* **2022**, *118*, No. 103329.

(17) Köster, M.; Thommes, M. In-Line Dynamic Torque Measurement in Twin-Screw Extrusion Process. *Chem. Eng. J.* **2010**, *164* (2–3), 371–375.

(18) Villberg, K.; Veijanen, A. Analysis of a GC/MS Thermal Desorption System with Simultaneous Sniffing for Determination of off-Odor Compounds and VOCs in Fumes Formed during Extrusion Coating of Low-Density Polyethylene. *Anal. Chem.* **2001**, *73* (5), 971–977.

(19) Lecun, Y.; Bengio, Y.; Hinton, G. Deep Learning. *Nature* **2015**, *521*, 436–444.

(20) Schuster, M.; Paliwal, K. K. Bidirectional Recurrent Neural Networks. *IEEE Trans. Signal Process.* **1997**, *45* (11), 2673–2681.

(21) Tominaga, A.; Sekiguchi, H.; Nakano, R.; Yao, S.; Takatori, E. Advanced Recycling Process for Waste Plastics Based on Physical Degradation Theory and Its Stability. *J. Mater. Cycles Waste Manag.* **2019**, *21* (1), 116–124.

(22) Patel, A. D.; Schyns, Z. O. G.; Franklin, T. W.; Shaver, M. P. Defining Quality by Quantifying Degradation in the Mechanical Recycling of Polyethylene. *Nat. Commun.* **2024**, *15* (1), 1–8.

(23) Zhang, Z. L.; Zhang, H. D.; Yang, Y. L.; Vinckier, L.; Laun, H. M. Rheology and Morphology of Phase-Separating Polymer Blends. *Macromolecules* **2001**, *34* (5), 1416–1429.

(24) Hibi, Y.; Tsuyuki, Y.; Ishii, S.; Ide, E.; Naito, M. Decoding Thermal Properties in Polymer-Inorganic Heat Dissipators: A Data-Driven Approach Using Pyrolysis Mass Spectrometry. *Sci. Technol. Adv. Mater.* **2024**, *25* (1), n/a.

- (25) Shorten, C.; Khoshgoftaar, T. M. A Survey on Image Data Augmentation for Deep Learning. *J. Big Data* **2019**, *6* (1), 1–48.
- (26) Gao, B.-B.; Xing, C.; Xie, C.-W.; Wu, J.; Geng, X. Deep Label Distribution Learning with Label Ambiguity. *IEEE Trans. Image Process.* **2017**, *26* (6), 2825–2838.
- (27) Pan, S. J.; Yang, Q. A Survey on Transfer Learning. *IEEE Trans. Knowl. Data Eng.* **2010**, *22* (10), 1345–1359.
- (28) Vaswani, A.; Brain, G.; Shazeer, N.; Parmar, N.; Uszkoreit, J.; Jones, L.; Gomez, A. N.; Kaiser, Ł.; Polosukhin, I. Attention Is All You Need. *arXiv* 2017, PrePrint. DOI: 10.48550/arXiv.1706.03762.
- (29) Hibi, Y.; Uesaka, S.; Naito, M. A Data-Driven Sequencer That Unveils Latent “Codons” in Synthetic Copolymers. *Chem. Sci.* **2023**, *14* (21), 5619–5626.
- (30) Hibi, Y.; Uesaka, S.; Naito, M. Thermogravimetry-Synchronized, Reference-Free Quantitative Mass Spectrometry for Accurate Compositional Analysis of Polymer Systems without Prior Knowledge of Constituents. *Analyst* **2024**, *149* (17), 4388–4394.
- (31) Watanabe, R.; Nakamura, S.; Sugahara, A.; Kishi, M.; Sato, H.; Hagihara, H.; Shinzawa, H. Revealing Molecular-Scale Structural Changes in Polymer Nanocomposites during Thermo-Oxidative Degradation Using Evolved Gas Analysis with High-Resolution Time-of-Flight Mass Spectrometry Combined with Principal Component Analysis and Kendrick Mass Defect Analysis. *Anal. Chem.* **2024**, *96* (6), 2628–2636.
- (32) Ozawa, T.; Nakamura, S.; Sato, H.; Shinzawa, H.; Hagihara, H.; Watanabe, R. High-Resolution TG-TOFMS Coupled with Principal Component Analysis and Kendrick Mass Defect Analysis: Elucidation of Molecular-Scale Degradation Behavior of Glass Fiber Reinforced Polypropylene during Thermo-Oxidative Degradation. *Anal. Chem.* **2025**, *97*, 1665.
- (33) Hibi, Y. Reference-Free Quantitative Mass Spectrometry in the Presence of Nonlinear Distortion Caused by in Situ Chemical Reactions among Constituents. *Analyst* **2024**, *149* (21), 5320–5328.
- (34) Wang, Z. H.; Li, Y. T.; Wen, F. C. A Novel In-Line Polymer Melt Viscosity Sensing System of Integrated Soft Sensor and Machine Learning. *IEEE Sens. J.* **2023**, *23* (11), 12181–12189.